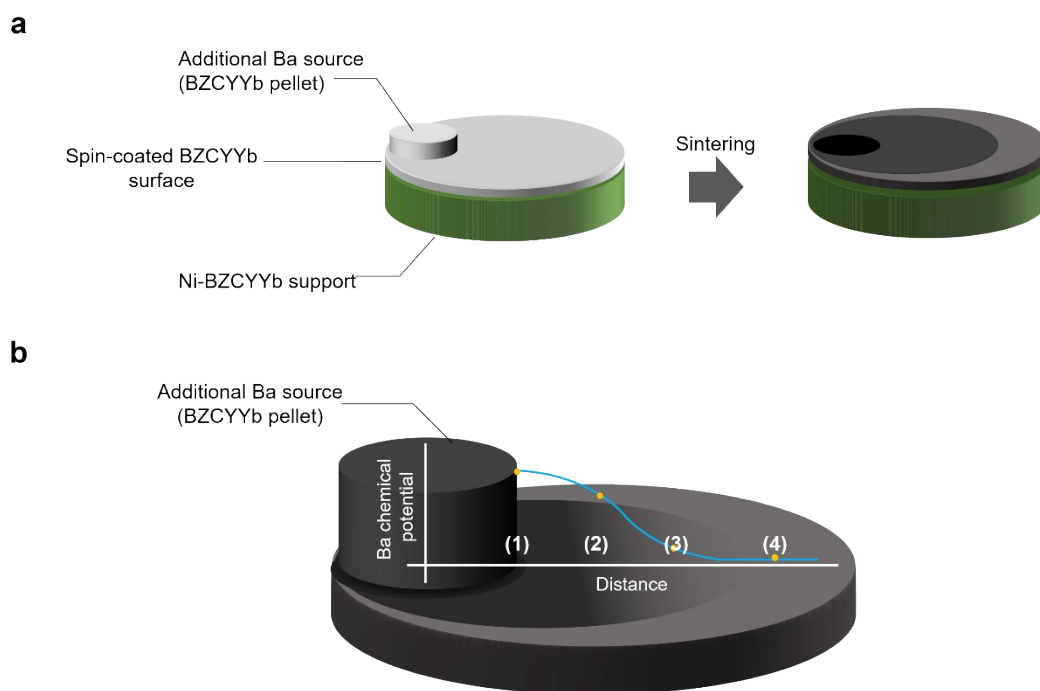**Supporting information**

Exceptionally high performance of protonic ceramic fuel cells with stoichiometric electrolytes

Mingi Choi, Jaedeok Paik, Donguk Kim, Deokyoon Woo, Jaeyeob Lee, Seo Ju Kim, Jongseo Lee, Wonyoung Lee*

School of Mechanical Engineering, Sungkyunkwan University (SKKU), Suwon 16419, South Korea

E-mail: leewy@skku.edu

\\

Supplementary Figure 1. Schematics of (a) the sample preparation, and (b) controlled chemical potential of Ba near the BZCYYb electrolyte surface in the lateral direction. Evaporated Ba from the additional Ba source diffuses from site (1) to site (4) following Fick's law of diffusion.

Supplementary Table 1. Representatively measured atomic concentration by EDAX, and calculated Ba/(Zr+Ce+Y+Yb) at the location of (1)-(4) in Supplementary Figure 1(b).

	Stoichiometric BZCYYb	Location			
		(1)	**(2)**	**(3)**	**(4)**
Ba at%	50.00	50.64	46.72	42.90	38.26
Zr at%	20.00	21.01	20.80	18.97	17.61
Ce at%	20.00	17.59	18.34	16.15	14.67
Y at%	5.00	5.96	8.08	13.31	16.37
Yb at%	5.00	4.80	7.77	8.66	13.08
Ba/(Zr+Ce+Y+Yb)	1.00	1.02	0.876	0.750	0.621

| Location	(1)	(2)	(3)	(4)
SEM observation				
Image process				
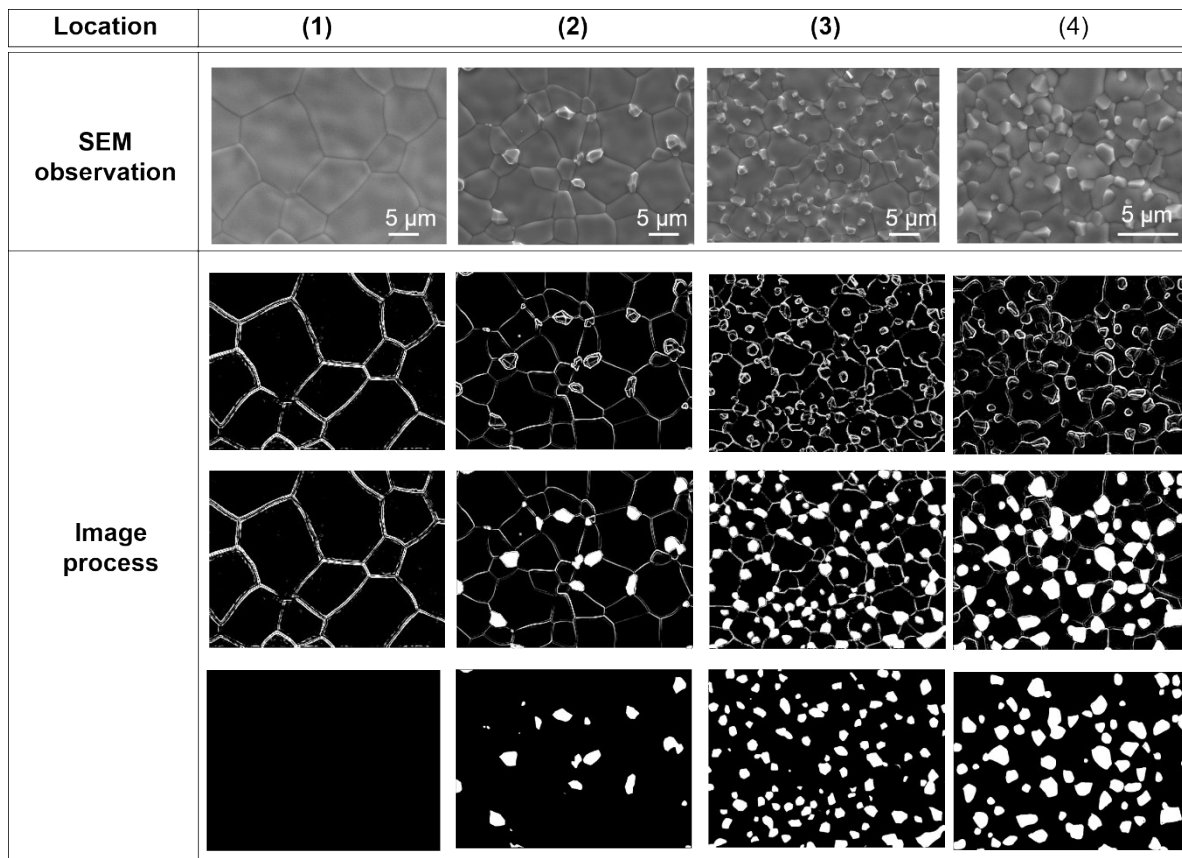
Supplementary Figure 2. Representative SEM images at the location of (1)-(4) in Supplementary Figure 1(b) and image processing procedure. Using the image processing software (Image J), the grain edges (or grain boundaries) were identified. Then, the secondary clusters were identified and marked as white based on the contrast difference between extruded clusters and the BZCYYb electrolyte surface. In this step, the grain size of the BZCYYb electrolyte was calculated excluding the secondary clusters. Then, the grain boundaries of the BZCYYb electrolyte were removed and the surface coverage of the secondary clusters was calculated by the equation as shown in below.

$$Surface\ coverage\ of\ secondary\ clusters\ (\%) = \frac{number\ of\ pixels\ for\ secondary\ clusters}{number\ of\ pixels\ for\ electrolyte\ surface} \times 100$$

.

Supplementary Table 2. Calculated grain size and surface coverage of secondary clusters at the location of (1)-(4) in Supplementary Figure 1(b).

Location	(1)	(2)	(3)	(4)
Grain size (µm)	9.57 ± 2.81	5.65 ± 1.75	4.42 ± 1.87	2.75 ± 0.87
Number of pixels for electrolyte surface	165,088	166,263	161,124	161,124
Number of pixels for secondary clusters	0	7,149	24,104	32,756
Surface coverage (%)	0	4.30	14.96	20.33
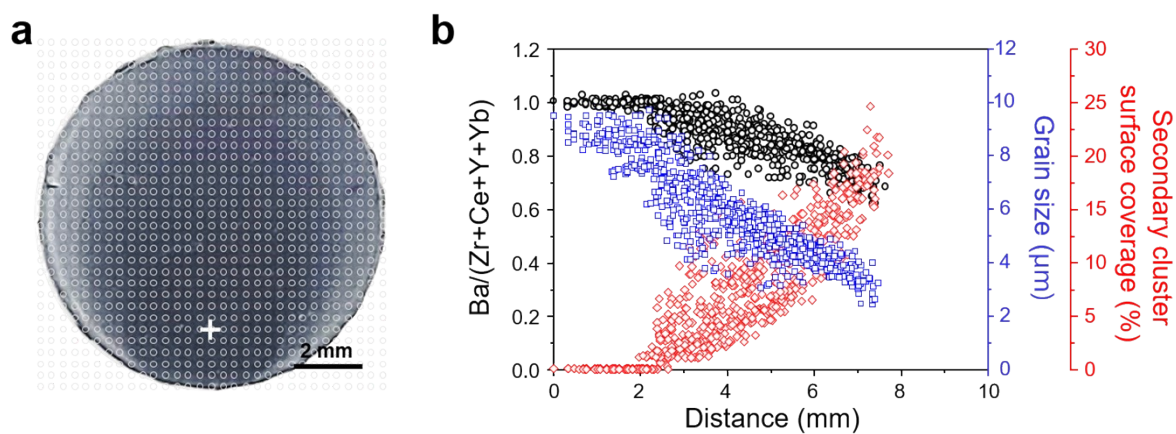
Supplementary Figure 3. (a) The optical image of the BZCYYb electrolyte after the sintering at 1500 °C for 5 h with the additional Ba source. (b) The Ba cation ratio, the average grain size, and the surface coverage of secondary clusters as a function of the distance which was measured between the center of the additional Ba source located on the BZCYYb electrolyte (a white cross mark in Supplementary Figure 4(a)) to the location where the measurement was performed.
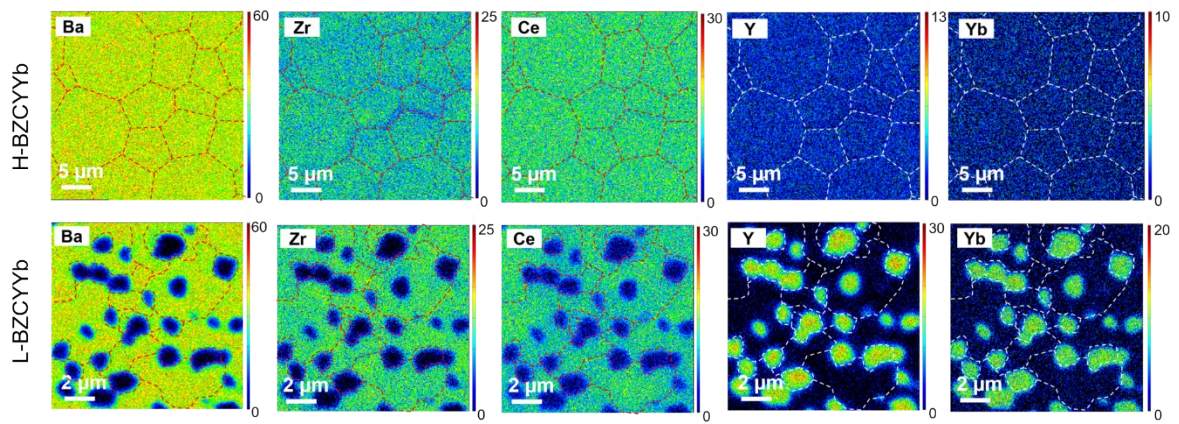
Supplementary Figure 4. FE-EPMA mapping of all constituent cations of H-BZCYYb and L-BZCYYb.

Supplementary Table 3. Conversion of the color intensity of each cation elemental map to the cation atomic concentration.

L-BZCYYb	Total color intensity in EDS mapping of each cation	Atomic ratio calculated by intensity in EDS mapping	Atomic ratio measured by EDS	Conversion factor
	Counts	%	%	
Ba	306,324	20.24	30.31	1.4973
Zr	285,614	18.88	22.66	1.2006
Ce	586,617	38.77	35.98	0.9280
Y	202,755	13.40	5.52	0.4121
Yb	131,734	8.71	5.52	0.6342
Sum of each column	1,513,044	100	100	

H-BZCYYb	Total color intensity in EDS mapping of each cation	Atomic ratio calculated by color intensity in EDS mapping	Atomic ratio measured by EDS area scanning	Conversion factor
	Counts	%	%	
Ba	720,367	33.28	52.76	1.5853
Zr	508,402	23.49	20.23	0.8615
Ce	446,885	20.64	20.31	0.9836
Y	191,709	8.85	2.49	0.2814
Yb	297,169	13.73	4.20	0.3061
Sum of each column	2,164,532	100	100	

Supplementary Table 3 shows an example of the conversion process of the color intensity of each cation in EDS elemental map to the cation concentration profile. First, the color intensity of each cation can be obtained from STEM-EDS elemental map in pixel units. The atomic ratio of each cation can be calculated by the ratio of the color intensity of each cation to the color intensity of all cations (Equation S1). Then, the atomic ratio of each cation calculated by the color intensity can be converted to the atomic concentration using the conversion factor, which is calculated by comparing the atomic ratio calculated by the color intensity and the atomic concentration by EDS measurement over the same area (Equation S2). Finally, the concentration profile of each cation in a thickness direction can be obtained from each row in STEM-EDS elemental map with a conversion factor, showing an average atomic concentration
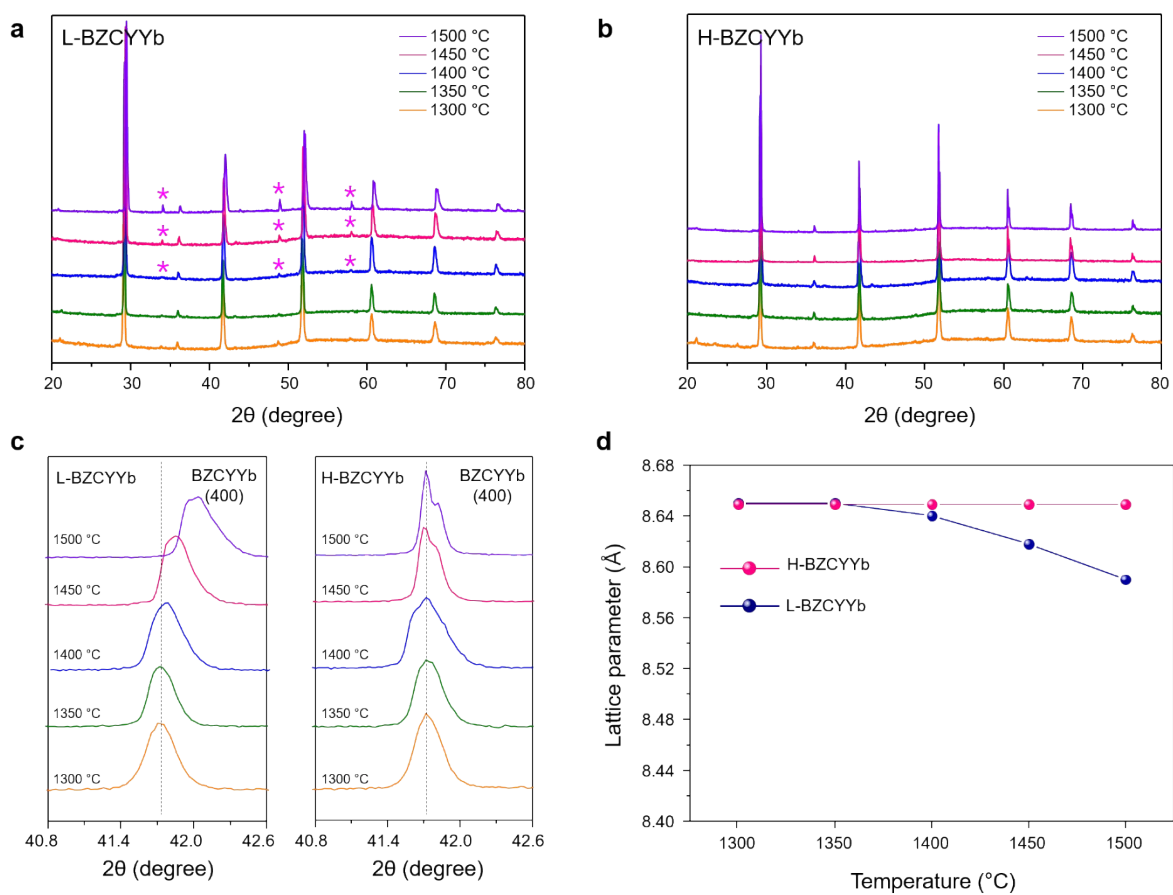
and the standard deviation as shown in Figures 2(c-d).

Equation S1:

$$\text{Atomic ratio calculated by color intensity in EDS mapping (\%)} = \frac{\text{Total color intensity in EDS mapping of each cation}}{\text{Sum of total color intesnity in EDS mapping of all cations}} \times 100 \text{ (\%)}$$

Equation S2:

$$\text{Conversion factor} = \frac{\text{Atomic ratio measured by EDS}}{\text{Atomic ratio calculated by color intensity in EDS mapping}}$$

Supplementary Figure 5. XRD patterns as a function of the sintering temperature of (a) L-BZCYYb and (b) H-BZCYYb. (c) BZCYYb(400) peak in XRD patterns, and (d) the lattice parameters.
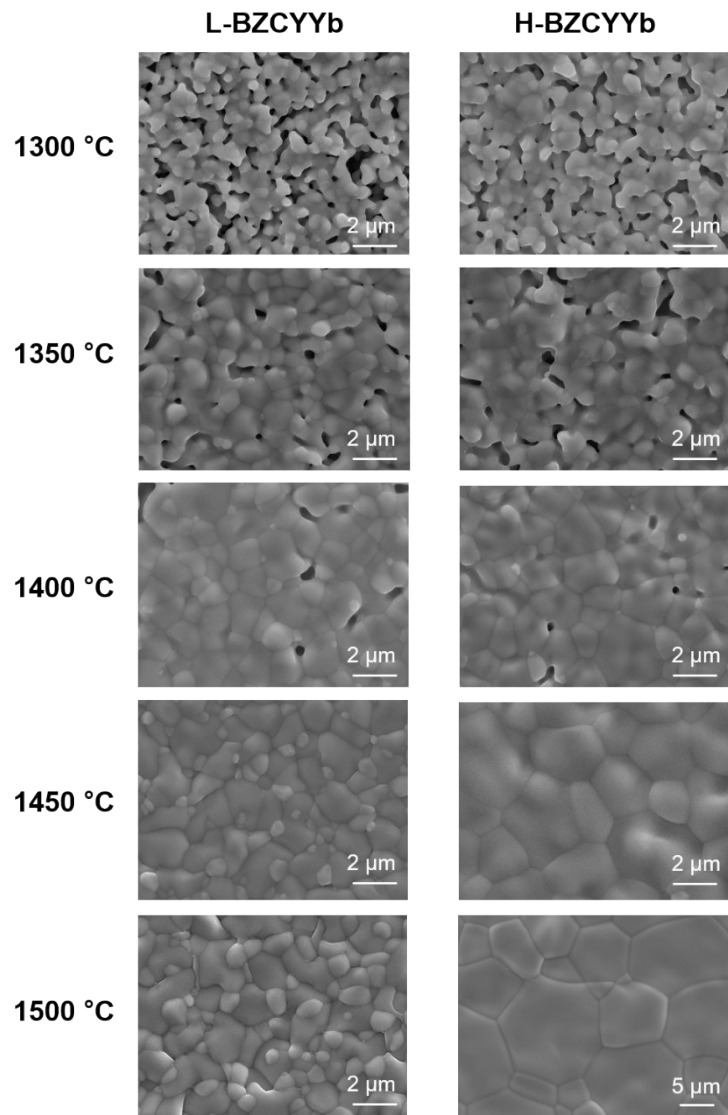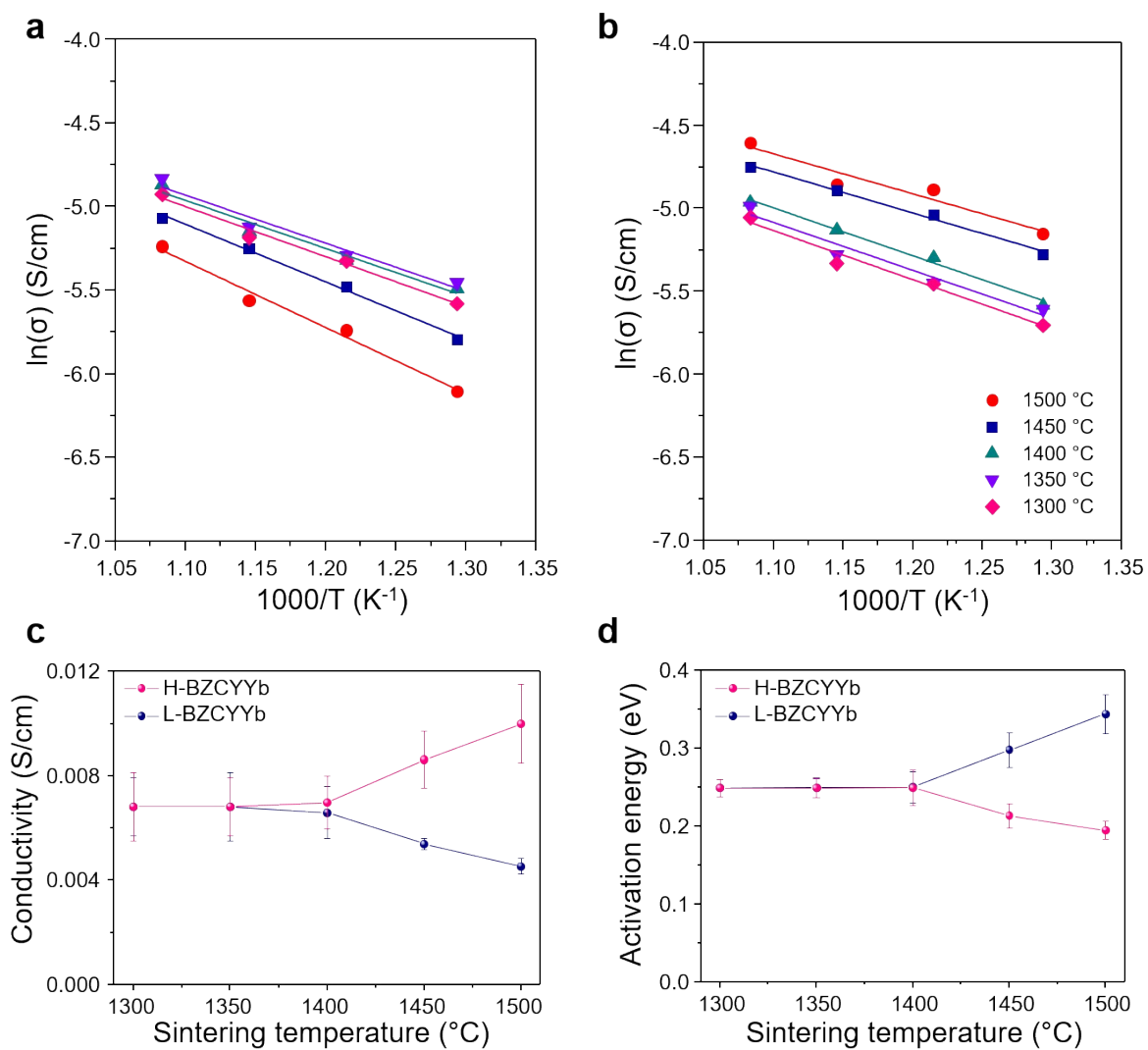
Supplementary Figure 6. SEM images of L-BZCYYb and H-BZCYYb obtained at sintering temperatures of 1300, 1350, 1400, 1450, and 1500 °C.
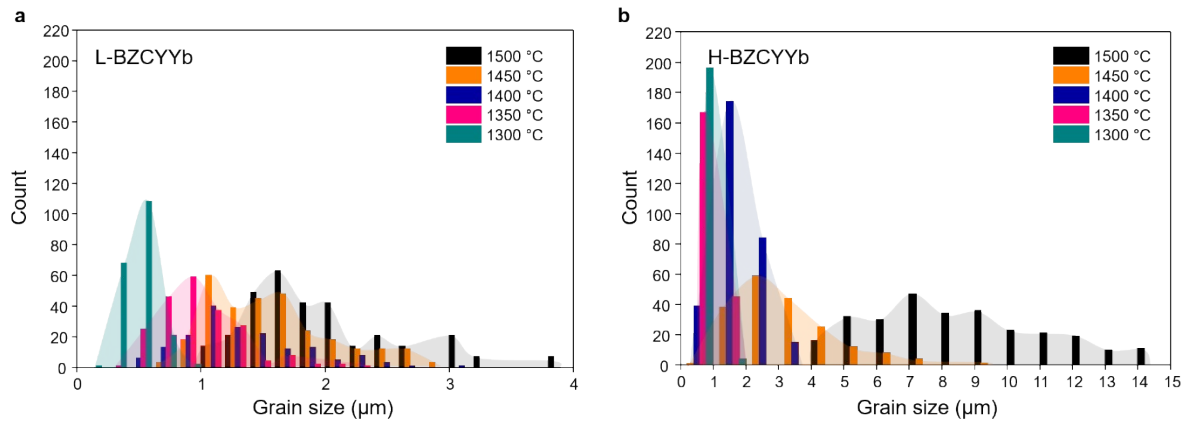
Supplementary Figure 7. Histograms of the grain size measured at sintering temperatures of 1300, 1350, 1400, 1450, and 1500 °C for (a) L-BZCYYb and (b) H-BZCYYb.

Supplementary Table 4. Average grain sizes of L-BZCYYb and H-BZCYYb at sintering temperatures of 1300, 1350, 1400, 1450, and 1500 °C

Sintering temperature (°C)	Grain size (µm)	
	L-BZCYb	H-BZCYYb
1300	0.46 ± 0.12	0.49 ± 0.16
1350	0.96 ± 0.34	0.82 ± 0.29
1400	1.33 ± 0.5	1.75 ± 0.71
1450	1.59 ± 0.49	3.25 ± 1.53
1500	2.73 ± 0.6	9.32 ± 2.63

Supplementary Figure 8. Arrhenius plot of (a) L-BZCYYb and (b) H-BZCYYb at sintering temperatures of 1300–1500 °C. (c) Proton conductivity measured at 650 °C and (d) activation energy as a function of the sintering temperature.
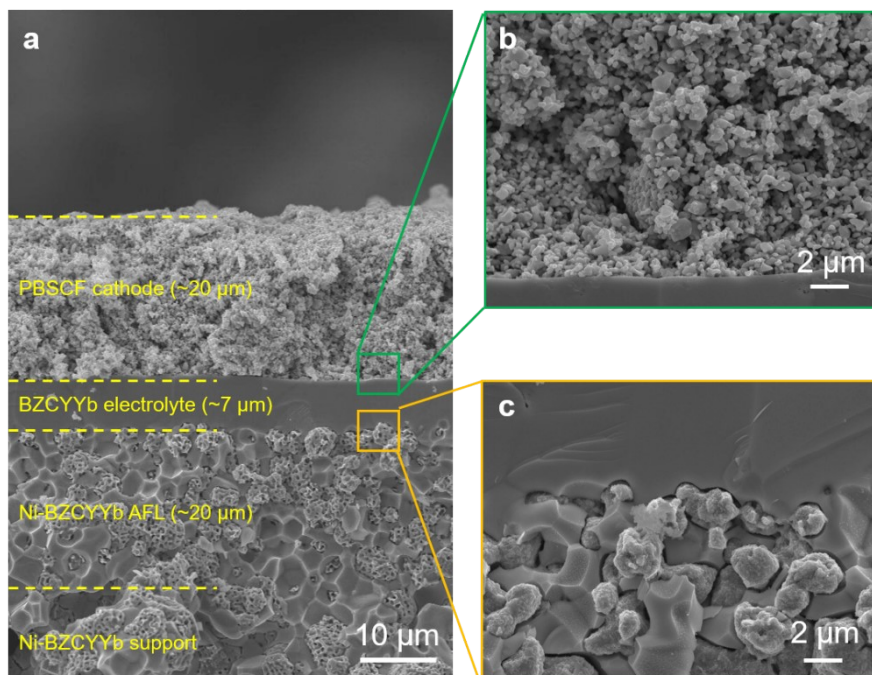
Supplementary Figure 9. Cross-sectional SEM image of (a) the single cell after reduction, (b) the interface between the cathode and electrolyte, and (c) the interface between the electrolyte and Ni–BZCYYb anode functional layer.
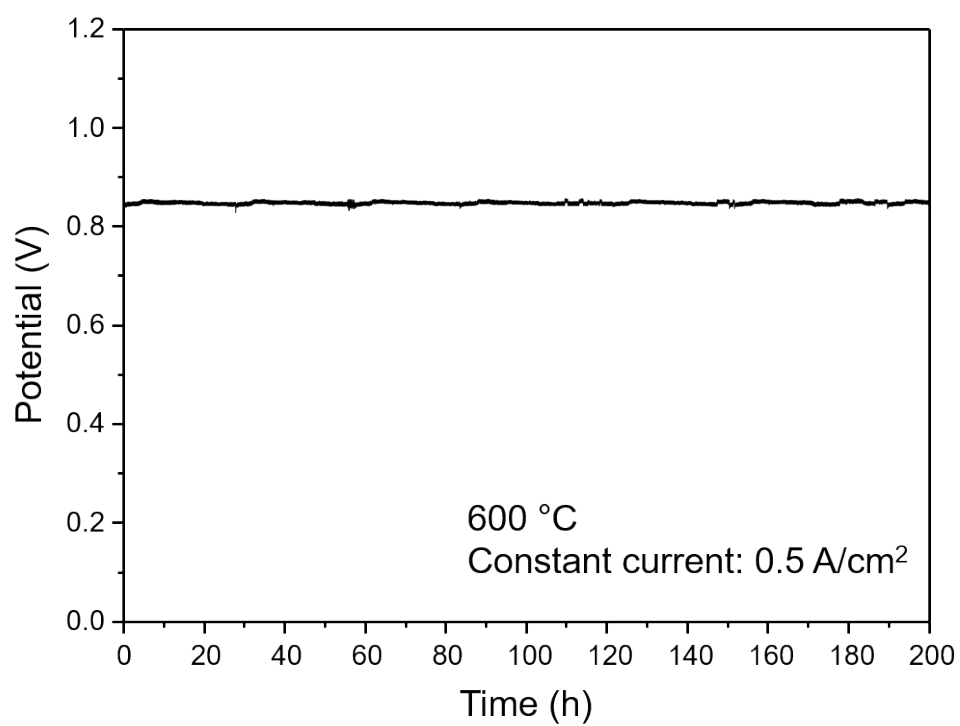
Supplementary Figure 10. Electrochemical stability evaluation of the H-BZCYYb cell at 600 °C for 200 h under a constant current density of 0.5 A/cm^2.
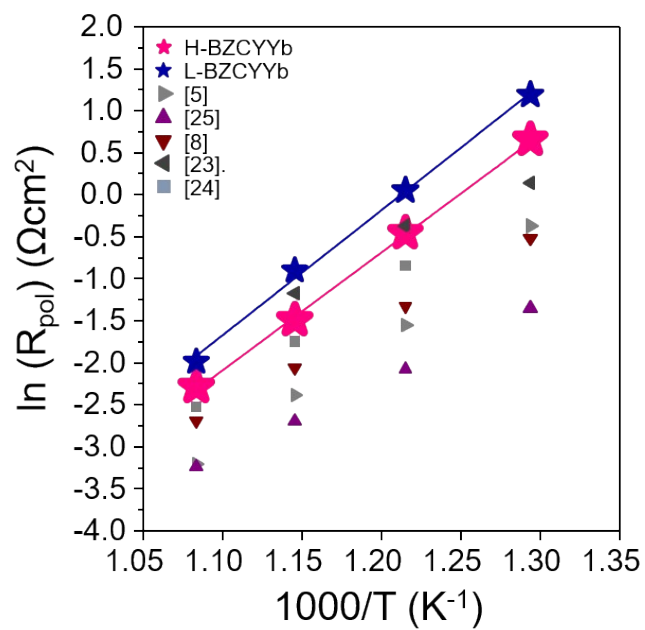
Supplementary Table 5. Comparison with previously reported PCFCs. We selected the results presented in papers published in the last 5 years with a reasonable power output.

| No	Components	Temperature (°C)	Area-specific ohmic resistance (ohm·cm²)	Area-specific polarization resistance (ohm·cm²)	Peak power density (mW/cm²)	Reference Information
1	Ni-BZCYYb / BZCYYb4411 / PBSCF	650	0.060	0.101	1903	In this study (H-BZCYYb)
		600	0.068	0.224	1474	
		550	0.082	0.628	1011	
		500	0.104	1.917	690	
2	Ni-BZCYYb / BZCYYb4411 / PBSCF	650	0.113	0.137	970	In this study (L-BZCYYb)
		600	0.160	0.405	693	
		550	0.195	1.052	534	
		500	0.252	3.288	342	
3	Ni-BCZY3 / BCZY3 / BSCF	650	0.075	0.040	1600	Ref. 5. An et al., Nat. Energy, 2018
		600	0.090	0.091	1306	
		550	0.122	0.211	900	
		500	0.173	0.689	535	
4	Ni-BZCYYb1711 / BZCYYb1711 / GCCCO-BZCYYb1711	650	0.132	0.039	1600	Ref. 25. Saqib et al., Energy Environ. Sci., 2021
		600	0.166	0.067	1160	
		550	0.201	0.125	770	
		500	0.241	0.258	480	
5	Ni-BZCYYb4411 / BZCYYb4411 / PBSCF (with PLD interlayer)	650	0.077	0.068	1400	Ref. 8. Choi et al., Nat. Energy, 2018
		600	0.090	0.128	1100	
		550	0.107	0.266	800	
		500	0.145	0.594	500	
6	Ni-BZCYYb4411 / BZCYYb4411 / PNC	600	0.200	0.31	611	Ref. 23. Ding et al., Nat. Commun., 2020
		550	0.290	0.69	450	
		500	0.410	1.15	310	
7	Ni-BZCYYb / BZCYYb4411 / PBSCF	650	0.098	0.080	1230	Ref. 24. Seong et al., Adv. Sci., 2021
		600	0.115	0.174	950	
		550	0.170	0.430	690	
		500	0.270	-	420	
8	Ni-BZY20 / BZY20 / BCFZY	600	-	-	660	Ref. 1. Duan et al., Nature, 2018
		550	-	-	525	
		500	-	-	422	

BZCYYb4411=$BaZr_{0.4}Ce_{0.4}Y_{0.1}Yb_{0.1}O_{3-\delta}$;   BZCYYb1711=$BaZr_{0.1}Ce_{0.7}Y_{0.1}Yb_{0.1}O_{3-\delta}$;   BCZY3=$BaCe_{0.55}Zr_{0.3}Y_{0.15}O_{3-\delta}$;   BZY20=$BaZr_{0.8}Y_{0.2}O_{3-\delta}$
BSCF=$Ba_{0.5}Sr_{0.5}Co_{0.8}Fe_{0.2}O_{3-\delta}$;   PBSCF=$PrBa_{0.5}Sr_{0.5}Co_{1.5}Fe_{0.5}O_{5+\delta}$;   GCCCO=$Gd_{0.3}Ca_{2.7}Co_{3.82}Cu_{0.18}O_{9-\delta}$;   PNC=$PrNi_{0.5}Co_{0.5}O_{3-\delta}$;
BCFZY=$BaCo_{0.4}Fe_{0.4}Zr_{0.1}Y_{0.1}O_{3-\delta}$;
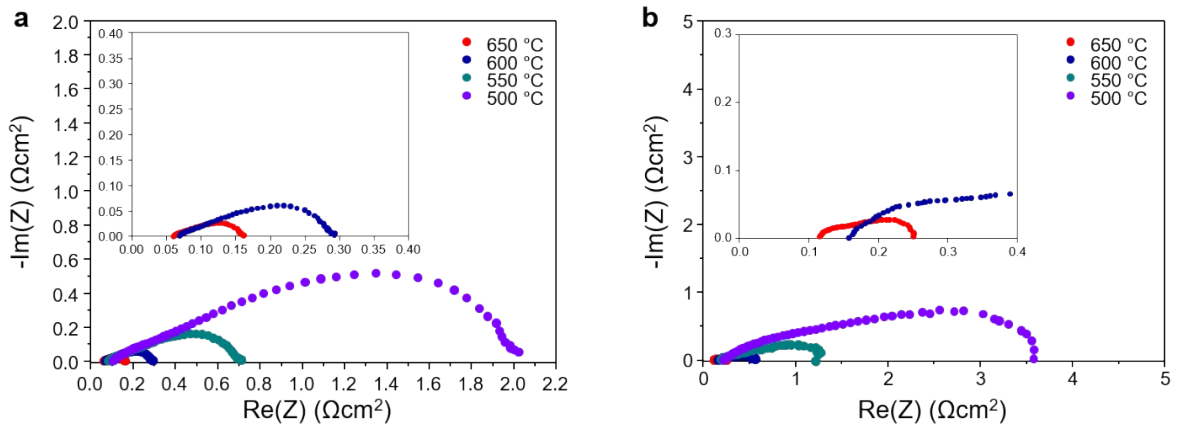
Supplementary Figure 11. Nyquist plots of (a) H-BZCYYb and (b) L-BZCYYb cells in the temperature range of 650–500 °C. The first intercept with the x-axis and the arc size represents the ohmic resistance and polarization resistance, respectively.

Supplementary Figure 12. Comparison of area-specific polarization resistance with previously reported PCFCs.
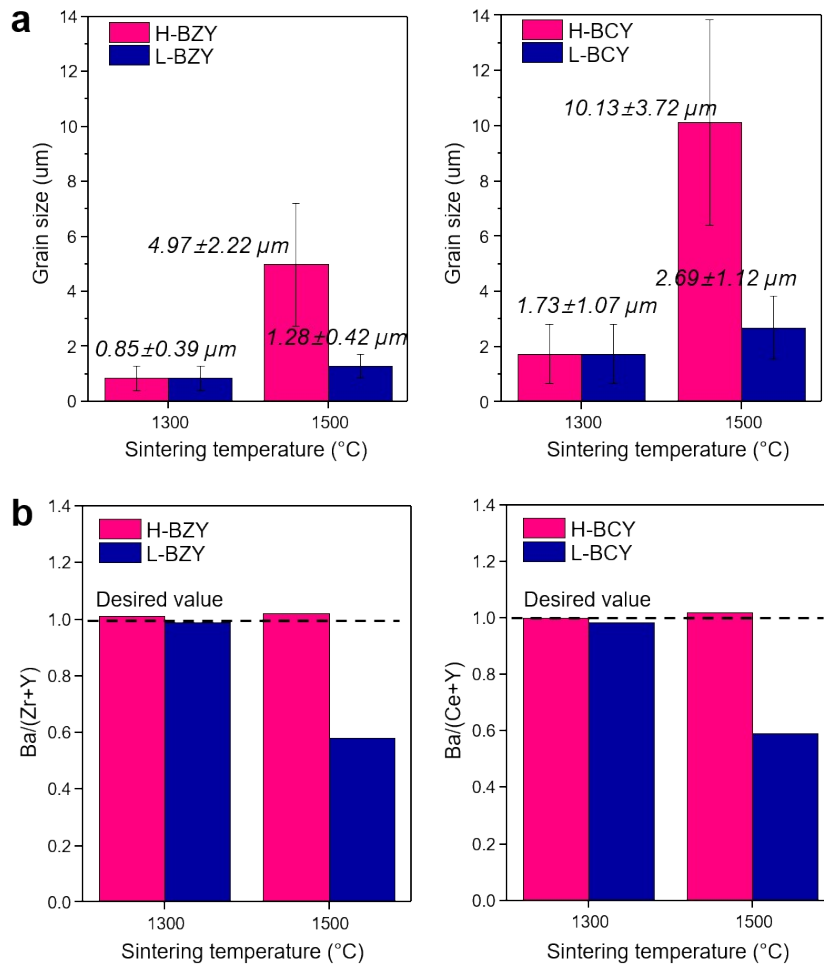
Supplementary Figure 13. (a) Average grain size and (b) Ba cation ratio of H-BZY/H-BCY and L-BZY/L-BCY with the sintering temperature of 1300 and 1500 °C.

$BaZr_{0.8}Y_{0.2}O_{3-\delta}$ (BZY) and $BaCe_{0.8}Y_{0.2}O_{3-\delta}$ (BCY)-based single cells were fabricated under the control of Ba chemical potential with the sintering temperature of 1300 °C and 1500 °C. With the sintering temperature of 1300 °C, there exists no noticeable difference in the grain size and chemical composition between H-BZY and L-BZY, and H-BCY and L-BCY. However, with the sintering temperature of 1500 °C, H-BZY/H-BCY show the significantly larger grain sizes with the desired chemical composition, while L-BZY/L-BCY show the significantly smaller grain sizes with Ba depletion.
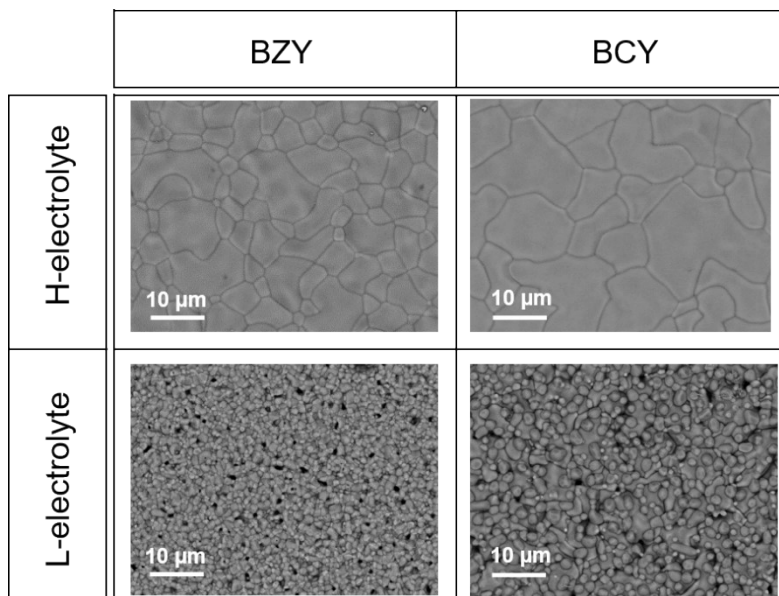
Supplementary Figure 14. SEM images of H-BZY/H-BCY and L-BZY/L-BCY electrolytes after sintering at 1500 °C.